Localized-mode evolution in a curved planar waveguide with combined Dirichlet and Neumann boundary conditions

O. Olendski
Atomic and Molecular Engineering Laboratory, Belarussian State University, Skarina Avenue 4, Minsk 220050, Belarus

L. Mikhailovska
Department of Higher Mathematics, Military Academy, Minsk 220056, Belarus

(Received 29 November 2002; published 27 May 2003)

We present a theoretical study of a planar waveguide with a uniformly curved section. Opposite sides of the channel satisfy different boundary conditions. It is shown that if the Dirichlet condition is applied to the inner side of the strip and the Neumann one to the outer wall, then properties of such a system in many respects resemble those with the Dirichlet requirements on both surfaces. Namely, in both cases a propagation threshold for the curved section is smaller than its counterpart for the straight channel. As a consequence, a localized mode exists with its energy below the propagation threshold of the straight waveguide. Analysis of such states is presented as a function of the bend parameters. For the transport in the fundamental mode an interaction of a quasibound level split off from the higher-lying threshold, with its degenerate continuum counterpart, causes a dip in the transmission. Such a resonance is characterized by a location of its zero minimum E_{min} and the half width Γ. Changing the bend angle and radius, one varies E_{min} and Γ. In particular, for some critical parameters of the bend it is possible to turn the half width to zero, i.e., to eliminate the dip in the transmission. This corresponds to the absence of the interaction between the split-off level and the continuum, and, consequently, to the formation of the true bound state in the continuum. Vortex structure of the currents flowing in the waveguide near the resonance is also shown to strongly resemble the analogous results for the Dirichlet case. It is pointed out that the properties of the waveguide with the Neumann inner condition and the Dirichlet outer one mimic the duct with the Neumann requirements on the two sides, since for both these cases the propagation threshold in the curved section is greater than in the straight channel.

DOI: 10.1103/PhysRevE.67.056625 PACS number(s): 41.20.Jb, 03.65.−w, 73.63.Nm, 84.40.Az

I. INTRODUCTION

Since a bent waveguide is frequently met with in many physical applications, its properties have been a subject of an intensive investigation for more than a century. Summary of this research in quantum theory can be found in Refs. [1,2], in radiophysics and electrodynamics in Refs. [3–5], in acoustics in Ref. [6], where many more references to the original publications are given. Other branches of science where a model of the bent waveguide is applied are elementary particle physics [7], quantum chemistry [8], and chemical physics [9,10]. Mathematically, wave dynamics in all these systems is described by the same type of the second-order differential equation—the Helmholtz equation:

$$\nabla^2\Psi(\vec{r})+k^2\Psi(\vec{r})=0. \tag{1}$$

For the spatially confined oscillations this equation should be complemented by the boundary conditions. If we assume that the fields do not penetrate outside of the waveguide, there are two types of them: Dirichlet one when the function Ψ vanishes at the boundaries $\mathcal{L}$ of the system,

$$\Psi|_{\mathcal{L}}=0, \tag{2}$$

and the Neumann one when a normal derivative of Ψ is zero at the confining walls,

$$\left.\frac{\partial\Psi}{\partial n}\right|_{\mathcal{L}}=0. \tag{3}$$

For example, for the de Broglie electronic wave which satisfies the Dirichlet conditions, $k=(2m_0E/\hbar^2)^{1/2}$ with m_0 being a particle mass and E being its energy. $\Psi(\vec{r})$ in this case is a wave function whose square determines probability of finding a particle at $\vec{r}$. For the electromagnetic or acoustic waves the wave vector k is the ratio of the frequency of oscillations ω and the speed of propagation in the space without the boundaries c_0: $k=\omega/c_0$, and $\Psi(\vec{r})$ is the electromagnetic or acoustic potential through which the electromagnetic fields or acoustic velocity and pressure are determined.

It is known that for the curved planar waveguide a propagation constant for the Dirichlet (Neumann) conditions is smaller (larger) than in the straight part [3,11]. Accordingly, for the Dirichlet case it is possible to have a wave propagating in the bend and exponentially vanishing in the straight arms. This leads to the existence of a bound state below the fundamental threshold for the waveguide with bend [12–14]. Levels split off from the higher-lying subbands, interfere destructively with their continuum counterpart leading to the steep dips in the transmission [15–17]. They are, in fact, quasibound states with a finite lifetime. However, for some parameters of the bend they transform into the true bound states in the continuum; as a result, a dip in the transmission vanishes with total propagation observable instead [17]. The-

oretical predictions of the bound states in the bent waveguides with the Dirichlet boundary conditions [12–14] were experimentally confirmed for the single- [18] and double-bend [19] structures.

On the other hand, the properties of a straight waveguide with the miscellaneous combination of mixed Dirichlet and Neumann boundary conditions on one or two walls were calculated recently by several authors [20–22]. It was predicted that for some configurations, such systems can support bound states below the fundamental propagation threshold. Bound states embedded into the continuum were found also for the straight acoustic duct with impurity [23]—Neumann analogy of a similar situation for the Dirichlet case [24].

In this paper, we study theoretically a curved planar waveguide with the different boundary conditions on the opposite confining walls. Such configuration appears as a natural generalization of the uniform conditions. Probably, one of the largest examples of a physical system satisfying such distribution of the boundary conditions is the Earth-ionosphere waveguide: it is known that for the very low frequencies the electromagnetic wave dynamics between the Earth and the ionosphere can be approximated, in the first approximation, as a propagation between the plates with the perfect electric (the Earth) and perfect magnetic (the ionosphere) conductors [25,26]. We show that the bent waveguide with the Dirichlet inner and Neumann outer conditions in many respects mimics the curved channel with the pure Dirichlet conditions. In particular, it possesses bound states below the propagation threshold of the straight guide. We calculate these levels' dependence on the bend angle and radius. For the propagation in the fundamental mode, similar to the pure Dirichlet case, a steep dip in the transmission is predicted to occur which is due to the interaction of the quasibound state split off from the higher-lying subband, with its degenerate continuum counterpart. Characteristics of this dip are thoroughly investigated; among others, it is shown that for some parameters of the bend a half width of the resonance turns to zero, which corresponds to the transformation of the quasibound level into the true bound state in the continuum. As we have stated above, the same behavior is characteristic for the Dirichlet conditions on both sides of the strip [17]. Another similarity between the two cases is the formation and evolution of the vortex structures near and at the resonance.

The paper is organized as follows. In Sec. II, our model is presented and a necessary formulation is briefly given. Section III is devoted to the presentation of the calculated results and their detailed physical interpretation for various parameters of the bend. Summary of the results is provided in Sec. IV.

II. MODEL AND FORMULATION

We consider an infinitely long quasi-one-dimensional waveguide of width d with a uniformly curved section of inner radius ρ_0 and angle ϕ_0 (Fig. 1). We assume hard-wall boundaries meaning that the fields do not penetrate out of the waveguide. On each of the sides we impose a uniform boundary condition—either the Dirichlet or Neumann one. For brevity, a case when a Dirichlet (Neumann) condition is

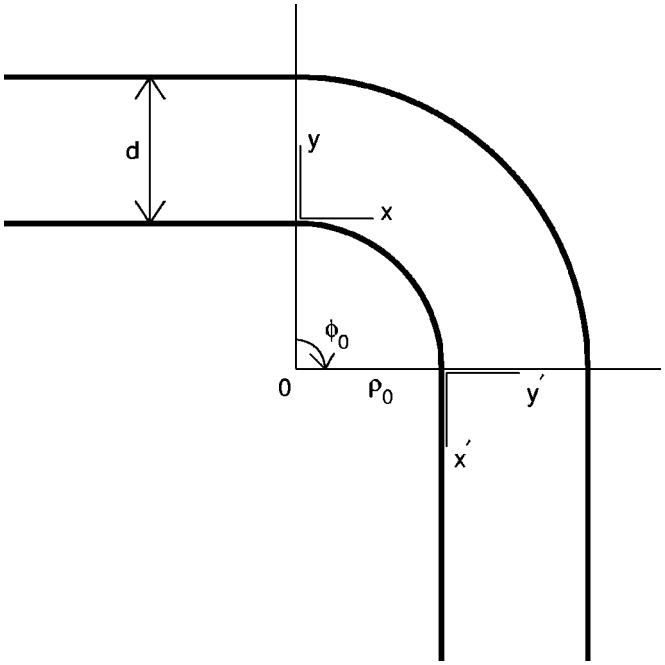

FIG. 1. Picture of the curved waveguide we study in this paper. Bend radius and angle are ρ_0 and ϕ_0, respectively. The width of the waveguide is a constant d. On each of the confining walls a uniform Dirichlet or Neumann boundary condition is imposed.

on the inner wall of the strip and the other condition on the outer side will be called below a DN (ND) case. Accordingly, the situation with the pure Dirichlet (Neumann) conditions on both sides of the channel is referred to as a DD (NN) configuration. Also, for definiteness, we will talk about the energy E, remembering that a transition, as described above, could be readily made to the frequencies ω. We measure all distances in the units of the waveguide width d and all energies in the units of $\pi^2\hbar^2/(2m_0d^2)$. Accordingly, in these units a wave vector k becomes $\pi E^{1/2}$, and its longitudinal component $k_n=\pi\sqrt{E-(n+1/2)^2}$. Also, our unit of time will be $2m_0d^2/(\pi^2\hbar)$.

For the scattering configuration, to the left of the bend, a solution to Eq. (1) is given as (we disregard the trivial z dependence)

$$\Psi(x,y)=\sum_{n=0}^{\infty}\{A_n\exp[i\pi\sqrt{E-(n+1/2)^2}x] + B_n\exp[-i\pi\sqrt{E-(n+1/2)^2}x]\}\chi_n(y), \quad (4)$$

with

$$\chi_n(y)=2^{1/2}\sin(n+1/2)\pi y \quad (5)$$

for the DN case, and

$$\chi_n(y)=2^{1/2}\cos(n+1/2)\pi y \quad (6)$$

for the ND case. Local Cartesian systems of coordinates (x,y) and (x',y') for the straight arms are shown in Fig. 1. Functions (5) and (6) have the corresponding eigenenergies which determine the propagation thresholds:

$$E_n=\left(n+\frac{1}{2}\right)^2. \tag{7}$$

After the bend one has

$$\Psi(x',y')=\sum_{n=0}^{\infty} C_n \exp[i\pi\sqrt{E-(n+1/2)^2}x']\chi_n(y'). \tag{8}$$

In Eq. (4) the terms with coefficients A_n describe the waves incident upon the bend, the terms with B_n are the modes reflected from (if $E>[n+1/2]^2$) or localized near it (for $E<[n+1/2]^2$). In the same way, in Eq. (8) the terms with positive $E-(n+1/2)^2$ are the modes propagating away from the curved area, and those with $E-(n+1/2)^2<0$ are the states bounded by it.

In a particular case, for A_n being a Kronecker symbol, $A_n=\delta_{nm}$, $m=0,1,\ldots$, due to the conservation law the following relation holds for the energies E such that $E>(m+1/2)^2$:

$$\sum_{n=0}^{\infty}\left(\frac{E-(n+1/2)^2}{E-(m+1/2)^2}\right)^{1/2}(|C_n|^2+|B_n|^2)\,\theta(E-(n+1/2)^2)=1. \tag{9}$$

$\theta(x)$ in Eq. (9) is a step function, and terms

$$\left(\frac{E-(n+1/2)^2}{E-(m+1/2)^2}\right)^{1/2}|C_n|^2 \quad \text{and} \quad \left(\frac{E-(n+1/2)^2}{E-(m+1/2)^2}\right)^{1/2}|B_n|^2$$

are, respectively, current transmission and reflection probabilities between subbands m and n.

Inside the bend, in the polar coordinate system with the pole coinciding with the center of the bend and the polar axis being the vertical junction between the straight and bent parts of the waveguide, solution of the Helmholtz equation reads

$$\Psi(\rho,\phi)=\sum_{n=1}^{\infty} R_n(\rho)[D_n\sin(\nu_n\phi)+F_n\cos(\nu_n\phi)] \tag{10}$$

with $R_n(\rho)$ being a radial part of the wave function:

$$R_n(\rho)=Y_{\nu_n}(\pi E^{1/2}\rho_0)J_{\nu_n}(\pi E^{1/2}\rho)-J_{\nu_n}(\pi E^{1/2}\rho_0)Y_{\nu_n}(\pi E^{1/2}\rho) \tag{11}$$

for the DN case, and

$$R_n(\rho)=Y_{\nu_n}(\pi E^{1/2}(\rho_0+1))J_{\nu_n}(\pi E^{1/2}\rho)-J_{\nu_n}(\pi E^{1/2}(\rho_0+1))Y_{\nu_n}(\pi E^{1/2}\rho) \tag{12}$$

for the ND case. Here $J_\nu(x)$ and $Y_\nu(x)$ are the Bessel functions of the first and the second kind, respectively [27], and ν_n is the nth root of the equation

$$J_\nu(\pi E^{1/2}\rho_0)Y'_\nu(\pi E^{1/2}(\rho_0+1))-Y_\nu(\pi E^{1/2}\rho_0)\times J'_\nu(\pi E^{1/2}(\rho_0+1))=0 \tag{13}$$

for the DN configuration, and

$$J'_\nu(\pi E^{1/2}\rho_0)Y_\nu(\pi E^{1/2}(\rho_0+1))-Y'_\nu(\pi E^{1/2}\rho_0)\times J_\nu(\pi E^{1/2}(\rho_0+1))=0 \tag{14}$$

for the ND case. A prime denotes a derivative of the function with respect to its argument. The left-hand sides of Eqs. (13) and (14) are considered as functions of variable ν, which is the index of the Bessel functions with all other parameters fixed. Accordingly, contrary to the system with a circular symmetry, in our case ν_n are not real integers. In the way similar to the pure Dirichlet [3,17] or Neumann [3,6,28] conditions, it can be shown that the solutions of Eqs. (13) and (14) are discrete and countably infinite, and only a finite number of the zeros are real, the remainder being purely imaginary [29]. As Eq. (10) shows, real zeros are naturally associated with the modes propagating inside the bend, and imaginary values describe the evanescent waves.

Equations (13) and (14) allow one also to define propagation thresholds in a continuously curved structure. Namely, putting in them the value of ν equal to zero, one finds the energies at which a new propagating channel opens up. We have

$$J_0(\pi E^{1/2}\rho_0)Y_1(\pi E^{1/2}(\rho_0+1))-Y_0(\pi E^{1/2}\rho_0)\times J_1(\pi E^{1/2}(\rho_0+1))=0 \tag{15}$$

for the DN case, and

$$J_1(\pi E^{1/2}\rho_0)Y_0(\pi E^{1/2}(\rho_0+1))-Y_1(\pi E^{1/2}\rho_0)\times J_0(\pi E^{1/2}(\rho_0+1))=0 \tag{16}$$

for the ND situation. These equations are considered as functions of E. For $\rho_0\to 0$, Eq. (15) transforms to

$$J_1(\pi E^{1/2})=0, \tag{17}$$

and Eq. (16) becomes

$$J_0(\pi E^{1/2})=0. \tag{18}$$

Equations of the type of Eqs. (15) and (16) are well known [27,30]. Their lowest solutions are shown in Fig. 2 as a function of the inner radius ρ_0. For comparison, least solutions for the DD,

$$J_0(\pi E^{1/2}\rho_0)Y_0(\pi E^{1/2}(\rho_0+1))-Y_0(\pi E^{1/2}\rho_0)\times J_0(\pi E^{1/2}(\rho_0+1))=0, \tag{19}$$

and NN cases,

$$J_1(\pi E^{1/2}\rho_0)Y_1(\pi E^{1/2}(\rho_0+1))-Y_1(\pi E^{1/2}\rho_0)\times J_1(\pi E^{1/2}(\rho_0+1))=0, \tag{20}$$

are also shown. These last two equations for the zero radius transform to Eqs. (18) and (17), respectively. It is seen that the solutions to Eqs. (15), (16), (19), and (20) for the large radii tend to the thresholds for the straight waveguide, as expected. For the zero radius the propagation thresh-

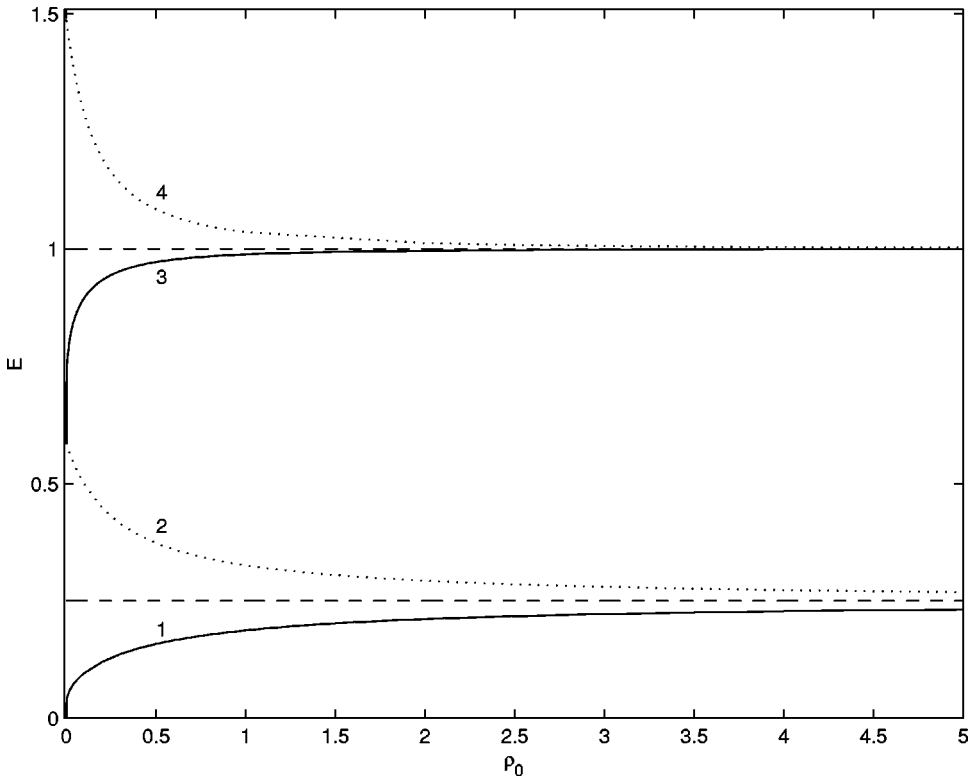

FIG. 2. Propagation thresholds in a continuously curved structure as a function of the bend radius ρ_0 where curve 1 is for the DN case, curve 2 is for the ND case, curve 3 depicts the DD situation, and curve 4 depicts the NN case. Thresholds for the straight waveguides are also shown where the lower dashed line $E=0.25$ corresponds to the mixed boundary conditions, and the upper one $E=1$ is for the pure Dirichlet or Neumann case.

old is equal to zero for the DN case, to $(j_{0,1}/\pi)^2 = 0.585\,959\,247\ldots$ for the ND and DD cases, and to $(j_{1,1}/\pi)^2 = 1.487\,594\,64\ldots$ for the NN situation, where $j_{\mu,n}$ is nth root of the function $J_\mu(x)$ [27,30]. For all values of the radius the thresholds for the DN (ND) case are smaller (larger) than its counterpart for the straight waveguide. In a sense, this makes them similar to the pure Dirichlet (Neumann) case. In particular, for the DN case it is possible to have a wave propagating in the curved section and decaying in the straight arms. As we stated above, for the pure Dirichlet situation this leads to the bound states with energies below the propagation threshold of the straight waveguide. It was proved recently [31] that this is also the case for the Neumann condition on the outer wall and the Dirichlet one for the inner side of the strip. In this case, instead of Eq. (4) we have evanescent modes only:

$$\Psi(x,y)=\sum_{n=0}^{\infty} A_n \exp[\pi\sqrt{(n+1/2)^2-E}x]\chi_n(y). \quad (21)$$

Matching wave functions at the junctions, one arrives either to the scattering matrix $\mathbf{S}(E)$ or to the equation determining eigenenergies of the bound states. For the fundamental mode $1/4 \leqslant E \leqslant 9/4$ the first diagonal scattering matrix element S_{11} determines the transmission T of the structure:

$$T=|S_{11}|^2. \quad (22)$$

III. RESULTS AND DISCUSSION

Since it is known [31] that for the DN case a bound state exists below the propagation threshold, we concentrate in this section just on this configuration of the boundary conditions. Figure 3 shows energies of the bound state as a function of the bend angle. For comparison, states for the pure Dirichlet conditions are also shown. A strong similarity between these two cases is seen. Energies monotonically decrease as ϕ_0 increases. They are also smaller for the smaller radius ρ_0.

Wave function of the bound state for $\rho_0=0.001$ and the right angle is shown in Fig. 4. It is symmetric with respect to the line $\phi=\phi_0/2$ and exponentially vanishes in the straight arms. In each of the cross sections, a minimal value of zero at the inner wall is accompanied by the maximum at the outer surface.

Figure 3 addressed the physically interesting situation of $0° \leqslant \phi_0 \leqslant 180°$. It is known that for the arbitrarily large angle the multiple bound states emerge for the DD configuration [18,32]. The same holds true for the DN case too, as Fig. 5 shows, where energies of the alternating symmetric and antisymmetric states are shown for the range $0° \leqslant \phi_0 \leqslant 900°$ with $\rho_0=0.1$. Again, a strong similarity with the pure Dirichlet conditions [32] is clearly seen. The lowest-energy state emerges at $\phi_0=0°$. This state is symmetric with respect to the middle of the bend, as it was discussed above. The next state that is an antisymmetric one, appears from the continuum at $\phi_0 \simeq 208.0°$. It is followed by the next symmetric state emerging at $\phi_0 \simeq 413.8°$, etc. On the quantitative note, we remark that for the DN case higher-lying bound states appear at the smaller angle than for the pure Dirichlet

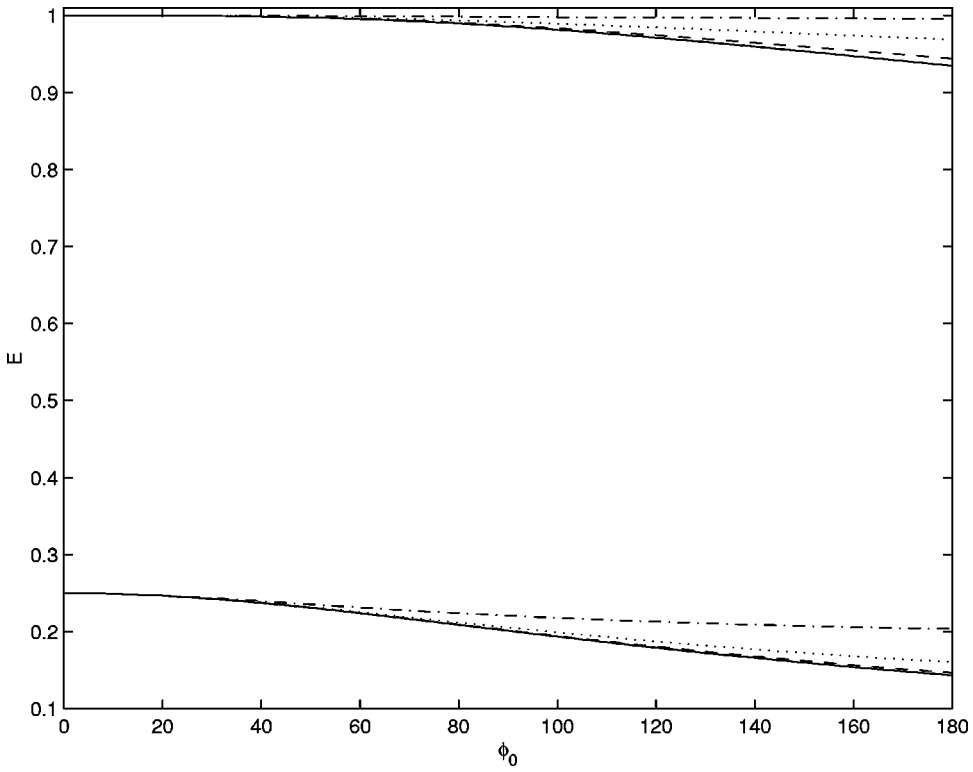

FIG. 3. Bound-state energies for the DN (lower curves) and DD (upper curves) cases as a function of the bend angle ϕ_0 for several values of the radius ρ_0: the solid line is for $\rho_0=0.001$, the dashed line is for $\rho_0=0.01$, the dotted line is for $\rho_0=0.1$, and the dash-dotted line is for $\rho_0=1$.

conditions. For example, for the latter case the first antisymmetric state appears at $\phi_0 \simeq 384.0°$.

For the pure Dirichlet conditions an approximation is used which maps the processes in the bent waveguide onto the dynamics in the straight channel with the additional attractive potential [18,33]. In the same way, we can say that for the mixed boundary conditions the bend creates some additional effective potential which is shifted to the wall with the Dirichlet condition. It is known that a bound state exists under these circumstances [21]. Contrary, for the ND case the effective potential in the straight waveguide is shifted to the plate with the Neumann condition and, as a result, a bound state cannot be formed [21].

Next, we turn to the scattering case. Figure 6 shows the transmission T as a function of energy E for $\rho_0=0.001$ and $\phi_0=180°$. Immediately after the lower threshold, from zero

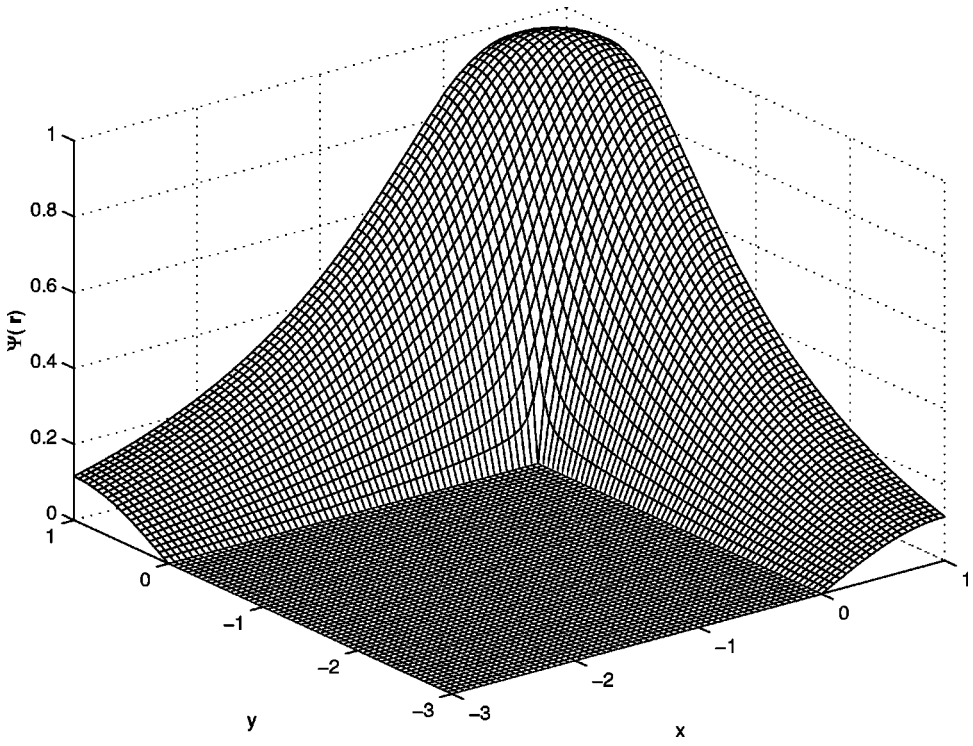

FIG. 4. Wave function (normalized to its maximum) of the bound state for $\rho_0=0.001$ and the right angle.

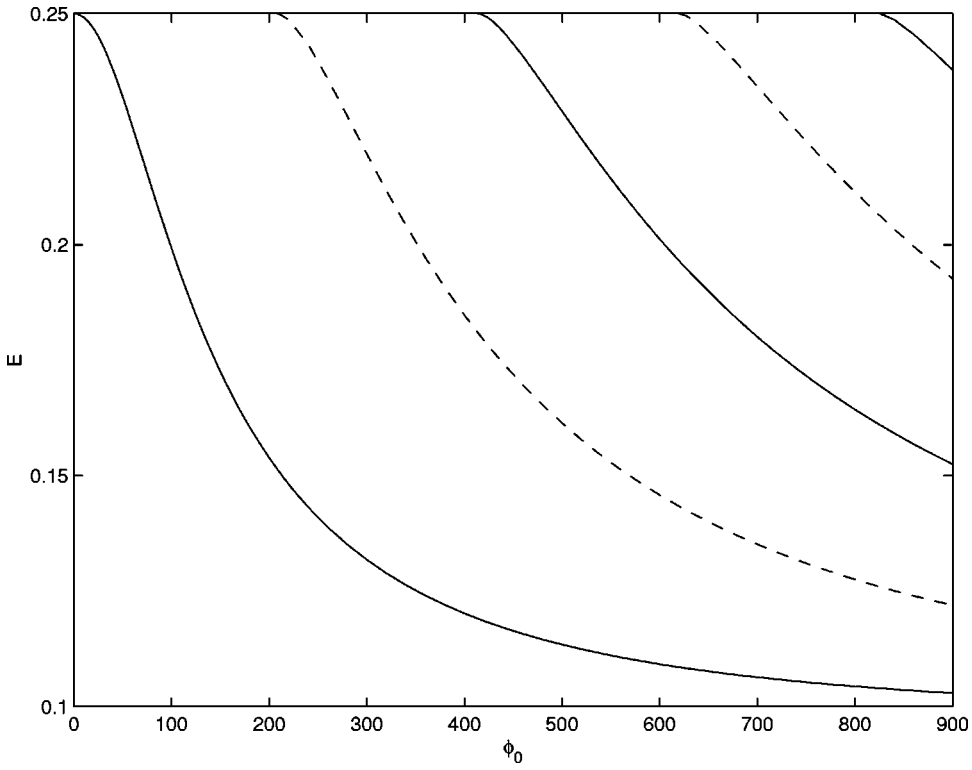

FIG. 5. Bound-state energies as a function of the angle ϕ_0 for $\rho_0=0.1$. Symmetric states are shown by the solid lines, and the antisymmetric ones by the dashed curves.

the transmission rapidly grows with energy. However, contrary to the pure Dirichlet case, one or several Breit-Wigner-like resonances show up immediately after the fundamental threshold. Location, width, and number of these resonances are determined by the bend parameters ρ_0 and ϕ_0. We attribute them to the propagating wave interaction with the effective potential of the bend in the presence of the upper Neumann plate. Second, similar to the DD case, we observe a steep dip in the transmission with the minimum of zero close to the first excited threshold. This dip is due to the splitting off of a quasibound level from the higher-lying subband. Mathematically, these states are formed as a result of the fact that the higher-lying solutions of Eqs. (15) and (19) are smaller than their counterparts for the straight wave-

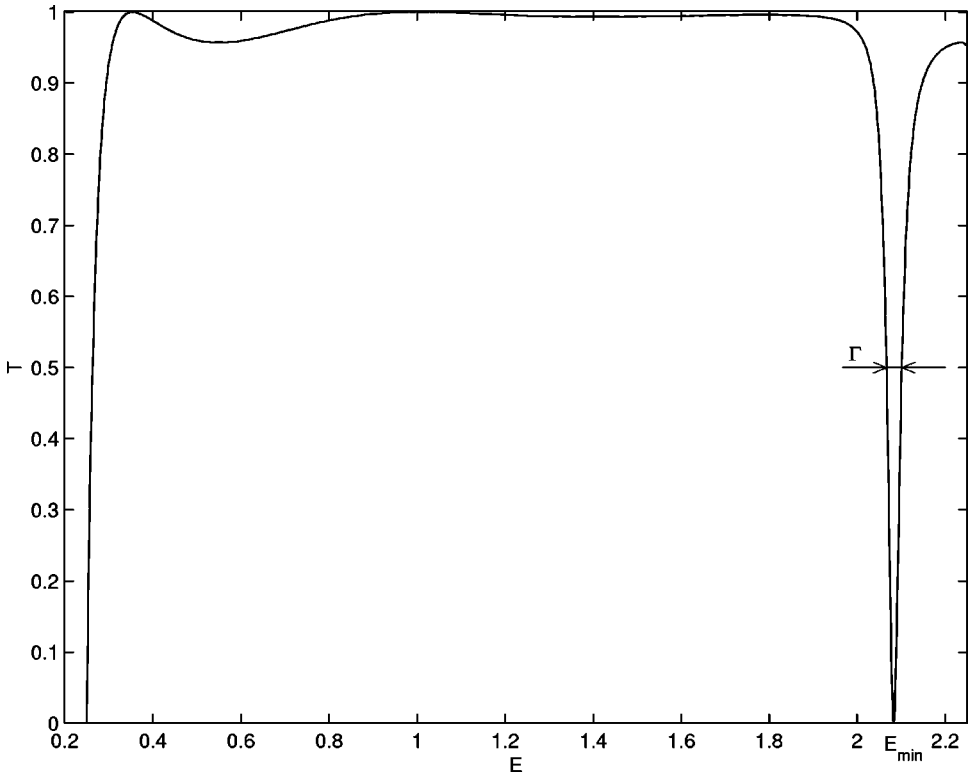

FIG. 6. Transmission T as a function of the energy E for $\rho_0=0.001$ and $\phi_0=180°$. Resonance near the upper threshold is characterized by its zero transmission location E_{min} and the half-width Γ.

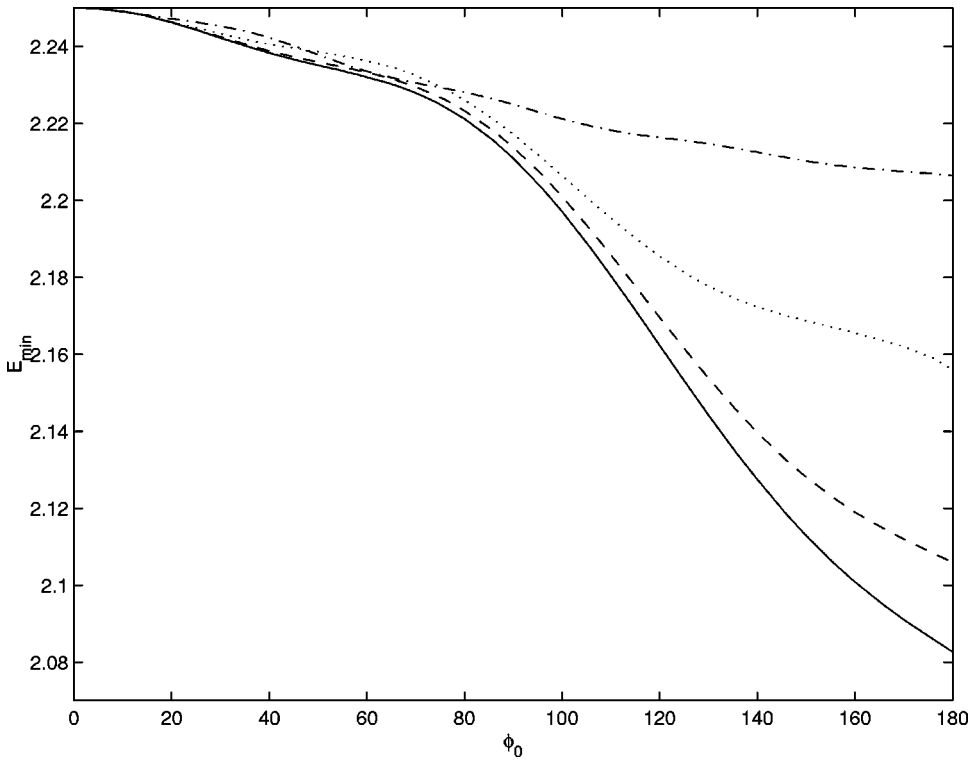

FIG. 7. Energies E_{min} as a function of the bend angle ϕ_0 for several values of the radius ρ_0. The convention of Fig. 3 is assumed.

guide. Imposing a bend, one mixes longitudinal and transverse motions in the waveguide that causes an intersubband interaction. As a result, an interference of this level with its degenerate continuum counterpart leads to the formation of the characteristic resonance with the energy of the zero minimum E_{min} and the half width Γ. These two quantities form a complex energy of the quasibound state:

$$E_{qb}=E_{min}-i\Gamma/2. \tag{23}$$

They are shown in Figs. 7 and 8, respectively. It is observed that the energies E_{min}, at which a complete interference blockade is achieved, decrease with the bend angle growing. However, contrary to the pure Dirichlet conditions [17], for

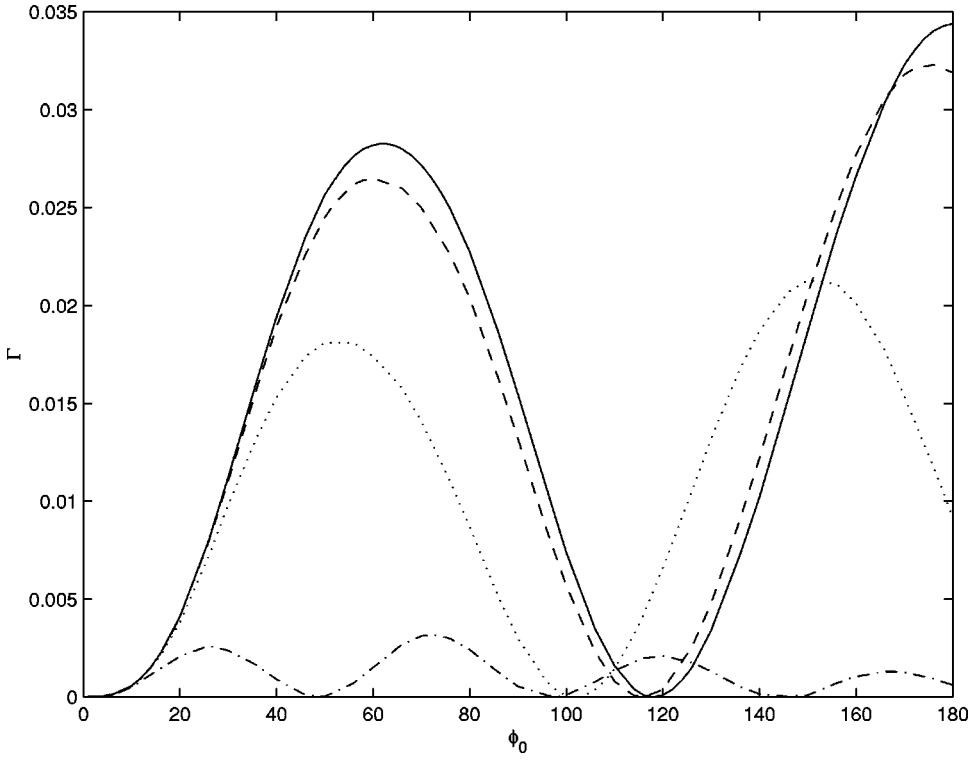

FIG. 8. Half-widths Γ as a function of the bend angle ϕ_0 for several values of the radius ρ_0. The same nomenclature as in Fig. 3 is used. Curve for $\rho_0=1$ has three zero minima on the ϕ_0 axis (excluding point $\phi_0=0$).

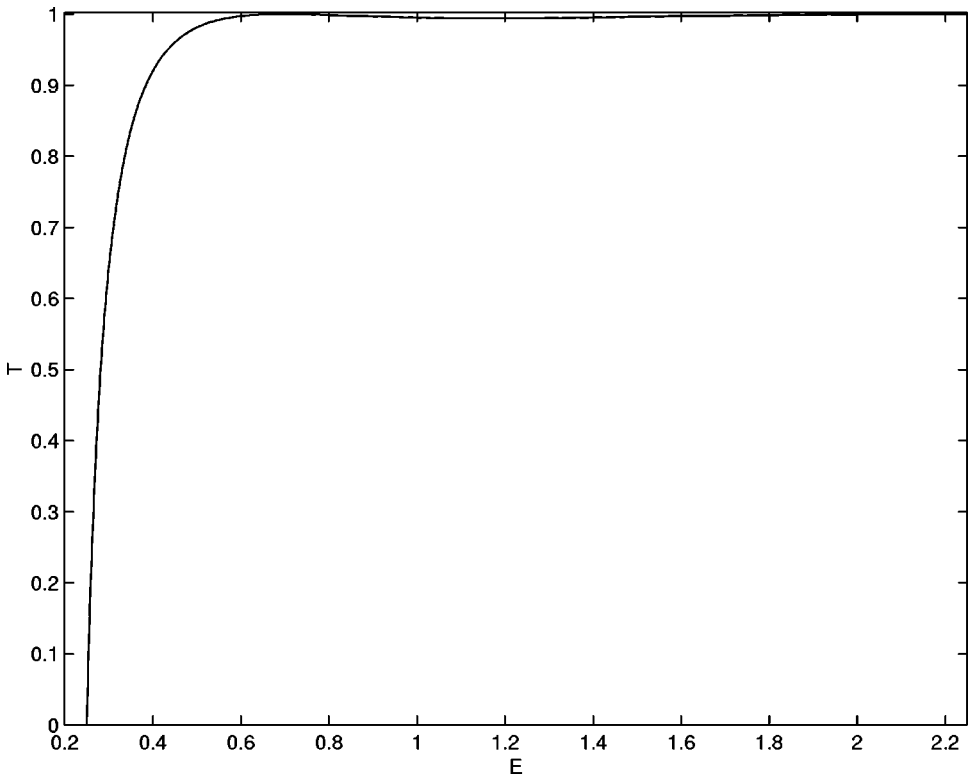

FIG. 9. Transmission T as a function of the energy E for $\rho_0=0.1$ and $\phi_0=101.9076°$. There is no dip in the transmission for these critical parameters of the bend.

some angle ranges the specific processes of the wave interference for the mixed conditions lead to the situation when the energy of the minimum increases if the bend radius ρ_0 decreases. The half width Γ, such as for the DD case [17], for the small and moderate angles increases from zero with ϕ_0, reaches maximum, decreases to the minimum of *zero*, after which the whole situation is repeated again. Zero value of the half width means that the dip in the transmission vanishes with a full propagation being observable instead. This is shown in Fig. 9 where the transmission T is plotted versus energy E for $\rho_0=0.1$ and $\phi_0=101.9076°$, i.e., when the corresponding Γ turns to zero in Fig. 8. Since a lifetime of a quasibound state τ is determined by Γ as

$$\tau=\frac{1}{\Gamma}, \tag{24}$$

a zero value of the half width means that the corresponding level has an infinite lifetime, i.e., it turns for these critical parameters of the bend into the true bound state in the continuum. Due to the resonant interference phenomena in the bend, such a state does not decay since it does not interact with its degenerate continuum counterpart. As a result, its wave function in the straight arms does not have a plane wave component, as it was the case for the quasibound level, exhibiting fading exponents only. Thus, bound states in the continuum, which were discussed for the first time soon after the formulation of quantum mechanics [34] and studied for the different physical systems with uniform Dirichlet [24,35–37,12,17] or Neumann [23] cases, are complemented by the new member—the curved planar waveguide with the Dirichlet inner and Neumann outer boundary conditions.

It is not surprising that the critical parameters at which the bound states in the continuum are formed are different from the DD distribution [17]. For example, instead of four true bound states in the continuum for the latter case with $\rho_0=1$, we observe only three such levels for $0°\leqslant\phi\leqslant180°$. However, all the pertaining discussion about their dependence on ρ_0 and ϕ_0 and a comparative analysis between these levels and the states split off from the fundamental mode remain valid in the considered case as well.

As a final example, we calculate a current density distribution for our system. For the case of the electron propagation the current density $\vec{j}$ is proportional to $\mathrm{Im}(\Psi\vec{\nabla}\Psi^*)$ [38]. The same holds true for the acoustic ducts when the mean sound energy flux is considered: $\vec{q}=p'\vec{v}$ with the pressure $p'=i\omega\rho_0\Psi^*$, acoustic velocity $\vec{v}=\vec{\nabla}\Psi$ and ρ_0 being here a density of the air [39]. Similar expressions for the Poynting vector involving Ψ and its complex conjugate are valid for the electromagnetic waves too. Figure 10 plots the current densities for the parameters of the bend from Fig. 6 and several energies E. When the energy is far away from the resonance value, one observes a longitudinal perfect laminar flow both in the straight arms as well as in the bend. For each of the cross sections, the current has a zero minimum on the inner wall and reaches maximum at the Neumann surface. When the energy comes closer to E_{min}, vortices start to form in the bend and its immediate neighborhood. For example, in Fig. 10(a) which corresponds to the transmission $T=0.9942$, the transverse component of $\vec{j}$ which was zero for the smaller energies is clearly observable near and inside the

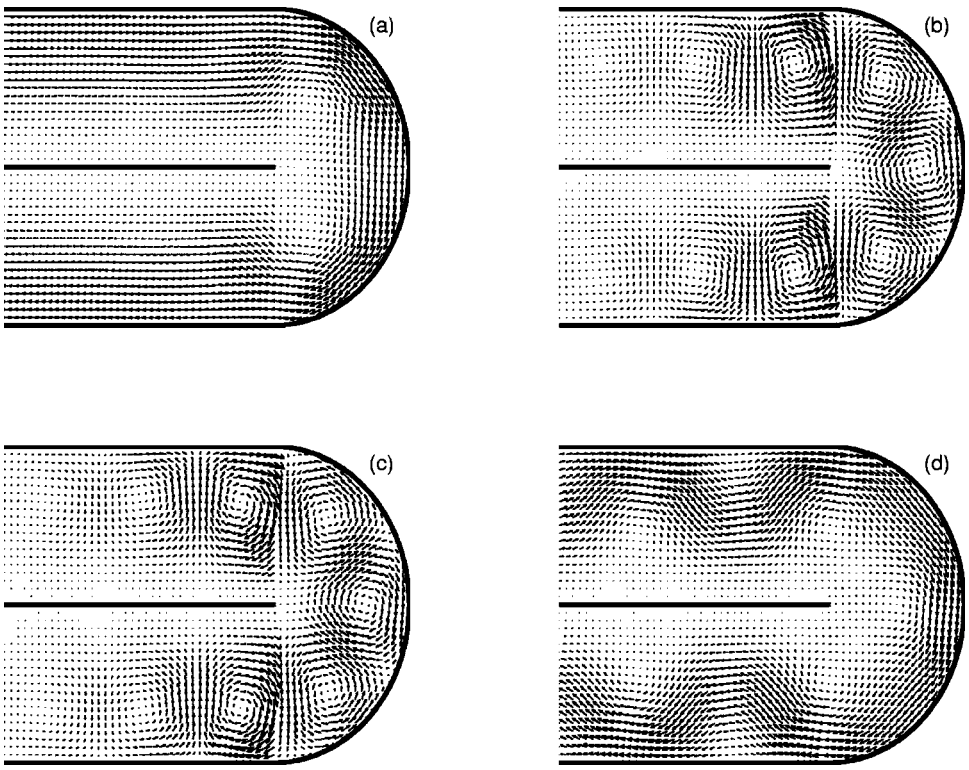

FIG. 10. Spatial distribution of the current density $\vec{j}$ for $\rho_0 = 0.001$, $\phi_0 = 180°$, and several values of the energy E: (a) $E = 1.9$, (b) $E = 2.0827$, (c) $E = 2.084$, (d) $E = 2.245$. Since the bend radius is very small, the distance between two parallel inner walls is not seen in the figure. Larger arrows denote higher currents. For each of the figures the currents are normalized with respect to their largest value.

curved section. Far away from the bend, the current still has a longitudinal component only. As we come closer to the resonant region, vortices develop in the waveguide. For example, Fig. 10(b) shows a vortex structure for the transmission $T = 4.8816 \times 10^{-6}$ just to the left from the resonance dip. Seeding of the vortices into the current density pattern is a result of the strong intersubband interaction which adds transverse components to the particle flow. Magnitude of the current in the vortices is of a few orders of magnitude larger than for the nonresonant values. Similar vortices for the pure Dirichlet boundary conditions were calculated before for the straight nonuniform [24,40–42] as well as for the bent waveguide without [43,44] and with the impurities [45,37]. For our structure, similar to the clean [10,43,46] and embedded-dot bent waveguide [37] for the DD case, the abrupt change of the rotation of the vortices is observable after passing the minimum transmission. For example, Fig. 10(c) shows $\vec{j}$ for $T = 5.399 \times 10^{-3}$ just to the right from the minimum. Compared to Fig. 10(b), the rotation of the vortices has changed to the opposite direction, which is retained for the higher transmissions when the vortices gradually resolve with the energies growing [Fig. 10(d)]. Formation and evolution of the vortices is a vivid example of the mixing by the bend of the different subbands and coupling of the longitudinal and transverse motion, which take place near the resonances.

IV. CONCLUDING REMARKS

We have considered theoretically a curved planar waveguide with the different boundary conditions on the opposite sides of the strip. The main result of our study consists in the fact that when the Dirichlet condition is applied to the inner boundary and the Neumann requirement to the outer surface, properties of the system are an almost exact replica of the wave behavior for the channel with the Dirichlet conditions on both sides. These similarities include the following: the existence of the bound state below the fundamental propagation threshold of the straight channel; interaction of the quasibound level in the fundamental propagation mode with its degenerate continuum counterpart, which causes a characteristic resonant profile; transformation, for some critical geometrical parameters of the bend, of this quasibound level into the true bound state in the continuum accompanied by the deletion of the dip which is substituted by the resonant tunneling through the bend; formation and evolution of the vortex structure for both configurations of the boundary conditions. Mathematically, this strong similarity stems from the fact that the solutions of the transcendental equations for the curved section for both cases are smaller than their counterparts in the straight channel, which physically means that it is possible to have a wave propagating in the bend and exponentially vanishing in the straight arms.

As we mentioned in the Introduction, different boundary conditions on the opposite sides are not a purely theoretical exotics; namely, it is the natural Earth-ionosphere waveguide which roughly obeys such demands. We believe that the other structures where the results predicted here can be verified are nanoelectronic or radio waveguides where the use is made of the properties of the ferrites [47] or superconductors [48].

It was also shown that for the ND case no bound state exists [31], similar to the pure Neumann conditions. Since we were interested in the localized modes and their evolution, we did not present here transmission characteristics for this case. However, the strong similarity between the ND and NN configurations, outlined in Sec. II, convincingly suggests

that they will be similar to the acoustic ducts [28,6]—in the same way as the DN case reminds the pure Dirichlet conditions. The bound state in the continuum may exist in the straight NN waveguide when the obstacle is inserted into it [23]. The same is true for the pure Dirichlet case [24]. Mathematically, an insertion of the scatterer into the waveguide leads to the additional term $-V(\vec{r})\Psi(\vec{r})$ in the left-hand side of Eq. (1), where for the existence of the localized mode in the continuum $V(\vec{r})$ should be negative (attractive interaction) for the DD case and positive (repulsive force) for the NN case. First theoretical and experimental study of the wave propagation in the curved NN channel with obstacle was performed about a quarter of century ago [49,50]. Though those who conducted that research do not mention this explicitly, we see from their results that they found Fano resonances [51] in the spectrum. For the pure Dirichlet case such resonances emerge and evolve as a result of the interaction of the negative $V(\vec{r})$ and the bend [37]. In the wake of the knowledge of the existence of bound states in the acoustic duct with the repulsive impurity [23], we deduce that a curved planar NN waveguide with obstacle exhibits Fano resonances due to the transformation of the true bound state in the continuum into the quasibound level. What happens in the bent waveguide with combined boundary conditions and embedded obstacle remains to be answered.

[1] P. Duclos and P. Exner, Rev. Math. Phys. **7**, 73 (1995).

[2] J.T. Londergan, J.P. Carini, and D.P. Murdock, *Binding and Scattering in Two-Dimensional Systems: Applications to Quantum Wires, Waveguides, and Photonic Crystals* (Springer-Verlag, Berlin, 1999).

[3] J.A. Cochran and R.G. Pecina, Radio Sci. **1**, 679 (1966).

[4] L. Lewin, D.C. Chang, and E.F. Kuester, *Electromagnetic Waves and Curved Structures* (Peter Peregrinus, Stevenage, UK, 1977).

[5] B.Z. Katsenelenbaum, L. Mercader del Río, M. Pereyaslavets, M. Sorolla Ayza, and M. Thumm, *Theory of Nonuniform Waveguides* (IEE, London, 1998).

[6] W. Rostafinski, *Monograph on Propagation of Sound Waves in Curved Ducts* (NASA Scientific and Technical Information Division, Washington, DC, 1991).

[7] F. Lenz, J.T. Londergan, E.J. Moniz, R. Rosenfelder, M. Stingl, and K. Yazaki, Ann. Phys. (N.Y.) **170**, 65 (1986).

[8] H. Eyring, J.E. Walter, and G.E. Kimball, *Quantum Chemistry* (Wiley, New York, 1944), Chap. 16.

[9] K.T. Tang, B. Kleinman, and M. Karplus, J. Chem. Phys. **50**, 1119 (1969).

[10] J.O. Hirschfelder and K.T. Tang, J. Chem. Phys. **64**, 760 (1976).

[11] C.P. Bates, Bell Syst. Tech. J. **49**, 2259 (1969).

[12] R.L. Schult, D.G. Ravenhall, and H.W. Wyld, Phys. Rev. B **39**, 5476 (1989).

[13] P. Exner, Phys. Lett. A **141**, 213 (1989); P. Exner and P. Šeba, J. Math. Phys. **30**, 2574 (1989); P. Exner, P. Šeba, and P. Štoviček, Czech. J. Phys., Sect. B **39**, 1181 (1989); Phys. Lett. A **150**, 179 (1990); M.S. Ashbough and P. Exner, *ibid.* **150**, 183 (1990); P. Exner, J. Math. Phys. **34**, 23 (1993); J. Phys. A **28**, 5323 (1995); P. Duclos, P. Exner, and D. Krejčiřík, Ukr. Fiz. Zh. **45**, 595 (2000) [Ukr. J. Phys. **45**, 595 (2000)]; Commun. Math. Phys. **223**, 13 (2001); P. Exner and D. Krejčiřík, J. Phys. A **34**, 5969 (2001).

[14] J. Goldstone and R.L. Jaffe, Phys. Rev. B **45**, 14100 (1992).

[15] F. Sols and M. Macucci, Phys. Rev. B **41**, 11887 (1990).

[16] K. Vacek, H. Kasai, and A. Okiji, J. Phys. Soc. Jpn. **61**, 27 (1992); K. Vacek, A. Okiji, and H. Kasai, Phys. Rev. B **47**, 3695 (1993).

[17] O. Olendski and L. Mikhailovska, Phys. Rev. B **66**, 035331 (2002).

[18] J.P. Carini, J.T. Londergan, K. Mullen, and D.P. Murdock, Phys. Rev. B **46**, 15538 (1992); **48**, 4503 (1993).

[19] J.P. Carini, J.T. Londergan, D.P. Murdock, D. Trinkle, and C.S. Yung, Phys. Rev. B **55**, 9842 (1997).

[20] W. Bulla, F. Gesztezy, W. Renger, and B. Simon, Proc. Am. Math. Soc. **125**, 1487 (1997).

[21] E.B. Davies and L. Parnovski, Q. J. Mech. Appl. Math. **51**, 477 (1998).

[22] J. Dittrich and J. Kříž, J. Math. Phys. **43**, 3892 (2002).

[23] D.V. Evans, C.M. Linton, and F. Ursell, Q. J. Mech. Appl. Math. **46**, 253 (1993); D.V. Evans, M. Levitin, and D. Vassiliev, J. Fluid Mech. **261**, 21 (1994).

[24] J.U. Nöckel, Phys. Rev. B **46**, 15348 (1992).

[25] K. Davies, *Ionospheric Radio* (Peter Peregrinus, London, 1991).

[26] S.F. Mahmoud, *Electromagnetic Waveguides: Theory and Applications* (Peter Peregrinus, London, 1991).

[27] *Handbook of Mathematical Functions*, edited by M. Abramowitz and I.A. Stegun (Dover, New York, 1964).

[28] A. Cummings, J. Sound Vib. **35**, 451 (1974); W.C. Osborne, *ibid.* **45**, 39 (1976); S. Félix and V. Pagneux, J. Acoust. Soc. Am. **110**, 1329 (2001).

[29] J.A. Cochran, J. Soc. Ind. Appl. Math. **12**, 580 (1964).

[30] E. Jahnke, F. Emde, and F. Lösch, *Tables of Higher Functions* (McGraw-Hill, New York, 1960).

[31] J. Dittrich and J. Kříž, J. Phys. A **35**, L269 (2002).

[32] K. Lin and R.L. Jaffe, Phys. Rev. B **54**, 5750 (1996).

[33] D.W.L. Sprung, H. Wu, and J. Martorell, J. Appl. Phys. **71**, 515 (1992); H. Wu, D.W.L. Sprung, and J. Martorell, Phys. Rev. B **45**, 11 960 (1992).

[34] J. von Neumann and E. Wigner, Z. Phys. **30**, 465 (1929).

[35] F.H. Stillinger and D.R. Herrick, Phys. Rev. A **11**, 446 (1975); H. Friedrich and D. Wintgen, *ibid.* **31**, 3964 (1985); **32**, 3231 (1985).

[36] C.S. Kim and A.M. Satanin, Zh. Éksp. Teor. Fiz. **115**, 211 (1999) [JETP **88**, 118 (1999)]; C.S. Kim, A.M. Satanin, Y.S. Joe, and R.M. Cosby, Phys. Rev. B **60**, 10 962 (1999); Zh. Éksp. Teor. Fiz. **116**, 263 (1999) [JETP **89**, 144 (1999)]; C.S. Kim, O.N. Roznova, A.M. Satanin, and V.B. Stenberg, *ibid.* **121**, 1157 (2002) [*ibid.* **94**, 992 (2002)].

[37] O. Olendski and L. Mikhailovska, Phys. Rev. B **67**, 035310 (2003).

[38] L.D. Landau and E.M. Lifshitz, *Quantum Mechanics (Non-Relativistic Theory)* (Pergamon, New York, 1977).
[39] L.D. Landau and E.M. Lifshitz, *Fluid Mechanics* (Pergamon, New York, 1959).
[40] C.S. Lent, Appl. Phys. Lett. **57**, 1678 (1990).
[41] S. Chaudhuri, S. Bandyopadhyay, and M. Cahay, Phys. Rev. B **45**, 11126 (1992); Z.-L. Ji and K.-F. Berggren, *ibid.* **45**, 6652 (1992); Z.-L. Ji, Semicond. Sci. Technol. **7**, 198 (1992).
[42] P. Exner, P. Šeba, M. Tater, and D. Vaněk, J. Math. Phys. **37**, 4867 (1996); P. Exner, P. Šeba, A.F. Sadreev, P. Středa, and P. Feher, Phys. Rev. Lett. **80**, 1710 (1998).
[43] K.-F. Berggren and Z.-L. Ji, Phys. Rev. B **47**, 6390 (1993).
[44] H. Wu and D.W.L. Sprung, Phys. Lett. A **183**, 413 (1993).
[45] E.N. Bulgakov and A.F. Sadreev, Zh. Tekh. Fiz. **71**, 77 (2001) [Tech. Phys. **46**, 1281 (2001)].
[46] E. Šimánek, Phys. Rev. B **59**, 10152 (1999).
[47] A.J. Baden Fuller, *Ferrites at Microwave Frequencies* (Peter Peregrinus, London, 1987).
[48] M. Tinkham, *Introduction to Superconductivity* (McGraw-Hill, New York, 1975).
[49] C.R. Fuller and D.A. Bies, J. Acoust. Soc. Am. **63**, 681 (1978); J. Sound Vib. **56**, 45 (1978).
[50] A. Cabelli, J. Sound Vib. **68**, 369 (1980).
[51] U. Fano, Phys. Rev. **124**, 1866 (1961).